

NASA/CR-97-

206826

INTERIM  
IN-43-CR  
OCIT

Semi-Annual Report Submitted to the  
National Aeronautics and Space Administration

For July - December, 1997

**Contract Number: NAS5-31370**  
**Land Surface Temperature Measurements**  
**from EOS MODIS Data**

MODIS Team Member  
PRINCIPAL INVESTIGATOR

ZHENGMING WAN

P.I.'s Address:

ZHENGMING WAN  
Institute for Computational Earth System Science  
University of California  
Santa Barbara, CA 93106-3060

phone : (805) 893-4541  
Fax no: (805) 893-2578  
Internet: wan@icess.ucsb.edu

# Land Surface Temperature Measurements from EOS MODIS Data

Semi-Annual Report  
For July - December, 1997

Zhengming Wan

## Abstract

We made modifications to the linear kernel bidirectional reflectance distribution function (BRDF) models from Roujean et al. and Wanner et al. that extend the spectral range into the thermal infrared (TIR). With these TIR BRDF models and the IGBP land-cover product, we developed a classification-based emissivity database for the EOS/MODIS land-surface temperature (LST) algorithm and used it in version V2.0 of the MODIS LST code. Two V2.0 LST codes have been delivered to the MODIS SDST, one for the daily L2 and L3 LST products, and another for the 8-day 1km L3 LST product. New TIR thermometers (broadband radiometer with a filter in the 10-13  $\mu\text{m}$  window) and an IR camera have been purchased in order to reduce the uncertainty in LST field measurements due to the temporal and spatial variations in LST. New improvements have been made to the existing TIR spectrometer in order to increase its accuracy to 0.2°C that will be required in the vicarious calibration of the MODIS TIR bands.

## Recent Papers Published and in Press

- Z. Wan and Z.-L. Li, "A physics-based algorithm for retrieving land-surface emissivity and temperature from EOS/MODIS data", *IEEE Trans. Geosci. Remote Sensing*, vol. 35, pp. 980-996, 1997.
- W. Snyder, Z. Wan, Y. Zhang and Y.-Z. Feng, "Requirements for satellite land surface temperature validation using a silt playa", *Remote Sens. Environ.*, vol. 61, pp. 279-289, 1997.
- W. Snyder and Z. Wan, "BRDF models to predict spectral reflectance and emissivity in the thermal infrared", *IEEE Trans. Geosci. Remote Sensing*, vol. 36, pp. 214-225, 1998.
- W. Snyder, Z. Wan, Y. Zhang and Y.-Z. Feng, "Classification-based emissivity for the EOS/MODIS land surface temperature algorithm", *Int. J. Remote Sensing*, in press 1998.
- Z. Wan, Y.-Z. Feng, Y. Zhang and M. D. King, "Land-surface temperature and emissivity retrieval from MODIS Airborne Simulator (MAS) data", to be in *Proceedings of the 7th JPL Airborne Earth Science Workshop*, Pasadena, CA, January 12-15, 1998.

## 1. New Developments for the MODIS LST Algorithm

Split-window LST methods need to use surface emissivity values in the two bands in the 10-13  $\mu\text{m}$  window. It is well known that the surface emissivity of a scene at the pixel scale of satellite observations, approximately 1km for AVHRR and MODIS, depends on not only the optical properties of the surface materials but also the surface roughness, structure, and proportions of all components in the scene. It is difficult over larger areas to measure the surface reflectance and/or emissivity of complex land cover types. This is especially true in the thermal infrared where both the reflected and emitted radiances are significant. We can find the spectral reflectance data of terrestrial materials in the literature and web sites. Most of these data are obtained from spectrometric measurements of small samples in laboratory such as by [Salisbury and D'Aria, 1992] and others. These include high-resolution spectra of single leaves, ice, water, snow, sand, different soil and rocks. In order to accurately estimate the scene emissivity from component emissivities and the parameters of surface structure and composition, we modified the linear kernel BRDF models [Roujean et al, 1992; Wanner et al, 1995] that were developed for the spectral range in visible and near infrared, and extend the spectral range into the thermal infrared. Because the details of the TIR BRDF kernel models are already described in a published paper [Snyder and Wan, 1998], we only summarize a few of its important features here. The model can reveal the angular variation in the scene emissivity. With foliage as modeled by the volumetric kernels, there is little angular dependence of the scene emissivity. On the other hand, the geometrical examples demonstrate that there may be a large angular dependence of the scene emissivity even with Lambertian components. This is because of structure - primarily because of the changing viewed proportions of the components. Another effect of going from components to the scene is that the spectral contrast is reduced because a mixture of components will have an averaging effect on the resulting spectrum.

With the combined use of the TIR BRDF kernel models and the IGBP land-cover classification, we developed a classification-based emissivity database for the MODIS generalized split-window LST algorithm [Wan and Dozier, 1996]. With the use of land-cover, snow-cover and vegetation index or time of year as inputs, our choice for combining and splitting 19 land-cover classes yields 14 emissivity classes. For example, we combine evergreen needle forest and green deciduous needle forest together into one emissivity class called green needle forest because it is not easy to discriminate these two types of forest with remote sensing data alone and they should have similar emissivity features. On the other hand, we

need to split the land-cover type of sparse shrublands into two emissivity classes, one for green sparse shrubs and another for senescent sparse shrubs because shrub has different emissivities when it changes from green to senescent. Based on several hundred spectra of natural materials, we believe that the 14 emissivity classes we chose can be discriminated and are a good balance between too many classes with similar emissivities, and too few, whereby emissivity accuracy is reduced. For each emissivity class, we designed a series of cases where the type of the components in the scene and the surface parameters can be changed in the appropriate ranges for this emissivity class. The band-averaged emissivities in the split-window bands can be estimated with the TIR BRDF kernel models for each cases. Finally, we can obtain the averaged values of the band emissivities at different viewing angles and their standard deviations for each emissivity class. Details are described in a paper in press [Snyder et al., 1998].

Table I shows the classification-based emissivity database used in the MODIS generalized split-window LST algorithm. Where  $\epsilon_{31}$  and  $\epsilon_{32}$  are band emissivities in MODIS bands 31 (at 11  $\mu\text{m}$ ) and 32 (at 12  $\mu\text{m}$ ), respectively,  $\text{rms\_m\_em}$  is the root of mean square of the mean emissivity of these two bands, and  $\text{rms\_d\_em}$  is the root of mean square of the emissivity difference in these two bands. Three more emissivity classes are included in Table I in addition to the 14 classes used in the above paper. Two of them for the land-cover type classified as urban and built-up in the green season and dry season. The components and corresponding proportions of the urban and built-up class are buildings 25%, road and parking 25%, bare soils/rocks 15%, sparse shrubs 10%, grass savanna 10%, broadleaf forest 10%, needle forest 5%. We also separate the emissivity class of snow/ice into two classes, one for dry/fine snow, another for medium and coarse snow and ice, for allowing the potential improvement to the LST algorithm if we can discriminate ice and dirty snow from dry/fine snow though it is not always possible. The values of  $\epsilon_{31}$ ,  $\epsilon_{32}$ ,  $\text{rms\_m\_em}$  and  $\text{rms\_d\_em}$  indicate that the split-window LST algorithm can retrieve LST accurately for water surface, dry/fine snow, dens vegetation areas in emissivity classes 4-8 because of the large emissivity values and small variations in the mean emissivities and the emissivity differences, and reasonable well for emissivity classes 3 and 10-12. However, the split-window LST algorithm cannot retrieve LST accurately for the last five classes, e.g., in the urban areas, and areas in the semi-arid and arid regions. In other words, for approximately one third of the global land surface, we will have real difficulty in the LST retrieval with the split-window method. For these areas, we will depend on the new day/night LST algorithm [Wan and Li, 1997] to retrieve the surface emissivities and temperatures simultaneously for improving the LST accuracy.

TABLE 1. The classification-based emissivity database for the MODIS split-window LST algorithm.

class	$\epsilon_{31}$	$\epsilon_{32}$	rms_m_em	rms_d_em	description
1	0.992	0.988	0.0049	0.0024	water surface
2	0.993	0.990	0.0023	0.0006	dry/fine snow
3	0.984	0.971	0.0069	0.0059	med/coarse snow & ice
4	0.989	0.991	0.0029	0.0005	green needle forest
5	0.987	0.990	0.0035	0.0015	green broadleaf forest
6	0.988	0.991	0.0039	0.0013	green doody savanna
7	0.987	0.991	0.0034	0.0014	green grass savanna
8	0.986	0.988	0.0040	0.0011	senescent needle forest
9	0.975	0.978	0.0095	0.0015	senescent woody savanna
10	0.977	0.982	0.0071	0.0022	organic bare soils
11	0.973	0.975	0.0115	0.0021	senescent grass savanna
12	0.968	0.971	0.0109	0.0038	senescent broadleaf forest
13	0.972	0.976	0.0134	0.0042	green sparse shrubs
14	0.970	0.975	0.0132	0.0044	senescent sparse shrubs
15	0.970	0.976	0.0139	0.0074	green urban & built-up
16	0.966	0.972	0.0117	0.0075	senescent urban & built-up
17	0.965	0.972	0.0148	0.0063	arid bare soil & rocks

## 2. V2 LST Code Delivery

We have delivered two V2.0 LST codes to the MODIS SDST (Science Data Support Team), one for the daily L2 and L3 (1km and 5km) LST products, and another for the 8-day 1km L3 LST product. New toolkits sdptk5.2v1.00, HDF4.1r1 and mapi2.2.1 were used in the code development for this delivery. Metadata and QA (quality assurance) attributes were also implemented in the V2 code. After new look-up

tables are established with the final spectral response functions at the MODIS system level, we will deliver V2.1 codes for the at-launch LST processing.

### 3. Improvements in TIR Instruments for the LST Validation

The experience gained from the field campaigns conducted for the validation of MODIS LST algorithms in 1995-1997 (some details shown in the paper to be presented at the 7th JPL Airborne Earth Science Workshop, January 12-15, 1998, in appendix A) shows that the temporal and spatial variations in the field measurements of LST are the major uncertainty in the LST validation. Recently we have made a great effort to reduce this uncertainty. We purchased 12 Heimann radiometers with a special window filter of 10-13  $\mu\text{m}$ . The effect of the large variation in emissivity below 10  $\mu\text{m}$  can be reduced by the use of this filter. We expect that the accuracy of the LST measurements can be improved by averaging the LST values from 12 Heimann radiometers well distributed over an area of 100 by 100m or 1 by 1km for comparison with LST values retrieved from MAS or MODIS data. We also purchased an IR camera from AGEMA Infrared Systems. There are 240 by 320 elements in this uncooling microbolometer-based IR camera. So we can easily place this IR camera on towers, low-level aircraft or balloons for measuring the temporal spatial LST distribution over test sites. Further improvements have been made to the existing scanning TIR spectrometer. The number of blackbodies in the front of the spectrometer is increased from two to four. One of the blackbodies is at the ambient temperature ( $T_{am}$ ), the second one at a temperature approximately 10  $^{\circ}\text{C}$  above  $T_{am}$ , the third one at 20  $^{\circ}\text{C}$  above  $T_{am}$ , and the fourth one at 10-15  $^{\circ}\text{C}$  below  $T_{am}$ . In this way, we can reduce the calibration error due to the non-linearity in the spectrometer response and reach the accuracy of 0.2  $^{\circ}\text{C}$  in the spectral ranges where the seven MODIS bands used in the MODIS LST algorithm are located. The spot size of the field-of-view of the scanning spectrometer is increased to 36cm from 12cm by placing it on a support structure 3m above the ground instead of 1m so that the surface sample measured by the spectrometer will better represent the surface condition of the test sites.

### 4. Anticipated Future Actions

In the first half of 1998, we will deliver all V2 codes for the at-launch LST processing, and will conduct a field campaign with MODIS Airborne Simulator flights and ground-based measurements at sites in Death Valley and Mammoth Lake area, California.

## REFERENCES

- Roujean, J., M. Leroy, and P. Deschamps, "A bidirectional reflectance model of the earth's surface for correction of remote sensing data," *J. Geophys. Res.*, vol. 97, pp. 20455-20468, 1992.
- Salisbury, J. W. and D. M. D'Aria, "Emissivity of terrestrial materials in the 8-14 $\mu$ m atmospheric window," *Remote Sens. Environ.*, vol. 42, pp. 83-106, 1992.
- Snyder, W. and Z. Wan, "BRDF models to predict spectral reflectance and emissivity in the thermal infrared," *IEEE Trans. Geosci. Remote Sens.*, vol. 36, no. 1, pp. 214-225, 1998.
- Snyder, W., Z. Wan, Y. Zhang, and Y.-Z. Feng, "Classification-based emissivity for the EOS/MODIS land surface temperature algorithm," *Int. J. Remote Sens.*, 1998.
- Wan, Z. and J. Dozier, "A generalized split-window algorithm for retrieving land-surface temperature from space," *IEEE Trans. Geosci. Remote Sens.*, vol. 34, no. 4, pp. 892-905, 1996.
- Wan, Z. and Z.-L. Li, "A physics-based algorithm for retrieving land-surface emissivity and temperature from EOS/MODIS data," *IEEE Trans. Geosci. Remote Sens.*, vol. 35, no. 4, pp. 980-996, 1997.
- Wanner, W., X. Li, and A. Strahler, "On the derivation of kernels for kernel-driven models of bidirectional reflectance," *J. Geophys. Res.*, vol. 100, pp. 21077-21089, 1995.

APPENDIX A

A paper to be presented at

The 7th JPL Airborne Earth Science Workshop

Pasadena, CA, January 12-15, 1998

## LAND-SURFACE TEMPERATURE AND EMISSIVITY RETRIEVAL FROM MODIS AIRBORNE SIMULATOR (MAS) DATA

Zhengming Wan, Yue-Zhong Feng, Yulin Zhang  
ICISS, University of California at Santa Barbara  
and Michael D. King  
NASA/Goddard Space Flight Center

### 1. INTRODUCTION

The Moderate Resolution Imaging Spectroradiometer (MODIS) has been developed as the keystone instrument for global studies of atmosphere, land, and ocean processes (Salomonson et al, 1989). MODIS, with 36 spectral channels, is scheduled to be launched in June 1998 on the EOS (Earth Observing System) AM-1 platform (King et al, 1995). In support of MODIS remote sensing algorithm development, the MODIS Airborne Simulator (MAS) has been developed for the NASA's high-altitude ER-2 research aircraft, and is an outgrowth of the development of the Wildfire infrared imaging spectrometer, originally designed for investigations of high-temperature terrestrial targets such as forest fires. King et al (1996) described its technical details, calibration methods, and evaluation of the MAS performance.

MAS in its June 1997 configuration has 50 narrowband channels shown in Table I in the spectral range between  $0.47\mu\text{m}$  and  $14.5\mu\text{m}$ , 10 of the shortwave channels ( $<2.5\mu\text{m}$ ) similar to the MODIS reflective channels, and 12 of the emissive channels similar to the MODIS thermal infrared (TIR) bands at approximately same wavelength locations including the seven MODIS TIR bands (bands 20, 22, 23, 29, and 31-33) used in the MODIS land-surface temperature (LST) algorithms. Beginning in January 1995, a 50-channel, 16-bit digitizer was used, which greatly enhanced the capability of MAS to simulate MODIS data over a wide range of environment conditions. The dynamic range of the TIR channels is wide enough to encompass cold cloud targets as well as warm terrestrial surface targets. MAS has a spatial resolution of 50m (pixel size) at the sea level as MAS is on the ER-2 research aircraft flying at altitude of 20km. Radiometric calibration of the shortwave MAS channels is obtained by observing laboratory standard integrating sphere sources on the ground before and after flight missions, while calibration of the infrared channels is performed in flight by viewing two onboard blackbody sources once every scan. The new calibration method (King et al, 1996) takes into account the effect of blackbody emissivity which is less than 1.0. We measured the spectral emissivity of the Krylon ultraflat black paint that was used to paint the MAS blackbodies, and applied this spectral emissivity and measured spectral response functions in the new calibration method for the MAS raw data in TIR channels.

In this paper, we briefly review the MAS flight missions for the validation of the MODIS LST algorithms in section 2, and the TIR instruments used in field measurements during the previous field campaigns in section 3. We present the preliminary results obtained from the calibrated MAS raw data in section 4, and describe the activities in the near future in section 5.

### 2. MAS MISSIONS FOR THE LST VALIDATION

MAS data have been acquired in multiple field campaigns at test sites (including Mono Lake and Mammoth Lake, and Death Valley) in California and Nevada since the first EOS Calibration/Validation Field Campaign conducted in Railroad Valley, Nevada, on 3 August 1995, as shown in Table II. The MAS mission number in the first column is given by the series number of the field campaign followed by D and N for daytime and nighttime MAS flights, respectively. Fortunately, the sites where we conducted ground-based measurements were in clear-sky conditions except the field campaign in the Mammoth Lake area in early April 1996. These clear-sky MAS data have been used for the validation of two MODIS LST algorithms. For land surfaces with known emissivities, a generalized split-window LST algorithm (Wan and Dozier, 1996) can be used to retrieve the surface temperature. A new physics-based day/night LST algorithm (Wan and Li, 1997) uses seven MODIS bands (three in the  $3.5\text{-}4.3\mu\text{m}$  region and four in the  $8\text{-}13.5\mu\text{m}$  region) for simultaneous retrieval of the land-surface temperature and emissivity. MAS on the ER-2 platform is the airborne sensor suitable for validating these two

MODIS LST algorithms because of its matched channel location, wide dynamic range, high calibration accuracy, and appropriate spatial resolution.

Large homogeneous test sites such as silt playas and inland lakes have been chosen because their in-situ surface temperatures and emissivities can be measured more accurately (Snyder et al, 1997a). We selected Railroad Valley, NV, as a test site for the validation of LST algorithms in the last three years because the uniform playa there is larger than 15 by 15km. As discussed in section 4, the standard deviation in the playa surface temperature is approximately 1 °C and 0.5 °C in day and at night, respectively. The purpose of the field campaign that we conducted at Mono Lake and Mammoth Lake, CA in April 1996 was to validate the LST algorithm for lake surface and snow cover. We conducted a field campaign at the flat alluvial fan called Devil's Golf Course in Death Valley, CA in March 1997. This alluvial fan is approximately 2km wide in the east-west direction and much longer in the north-south direction. Although the size of the alluvial fan is not large enough for the validation of LST algorithm for MODIS pixels, the diversity of rocks and the low vegetation coverage in Death Valley make it an ideal test site for the validation of the day/night LST algorithm for emissivity retrieval.

### 3. TIR INSTRUMENTS FOR FIELD MEASUREMENTS

In order to compare the LST values retrieved from MAS data, we need to measure the temporal and spatial variations in the land-surface temperature at the same viewing angle. We measure the land-surface temperature with three kinds of TIR instruments: thermistor with portable datalogger, hand-held infrared thermometer (broadband radiometer), and TIR scanning spectrometer. Thermistors are primarily for measurements of the temperature of water and playa 1-2mm beneath the surface. Broadband radiometers and TIR spectrometer are used for measurements of the surface temperature if the surface emissivity can be obtained from independent measurements. We used two kinds of broadband radiometers, one manufactured by Everest and another by Heimann, in our previous field campaigns. The TIR spectrometer (from MIDAC Corp.) equipped with InSb/MCT sandwich detector can provide radiance data at a selectable spectral resolution of 1 to 32 wavenumbers in the spectral range 3.5-14.5 $\mu$ m. Normally we select the 4 wavenumber resolution in our field measurements. At this spectral resolution, the speed of the spectrometer is 8 spectra per second. We made a series of custom improvements to this TIR spectrometer, including installation of a scanning mirror and two-three blackbody boxes in the front of the spectrometer. This TIR spectrometer with the scanning mirror can scan a range of angles to provide temporal and angular spectral surface radiance and atmospheric downwelling irradiance (with a diffuse reflector). The measured downwelling irradiance has been used in the atmospheric correction of the ground-based measurement data. These TIR instruments are calibrated with a full aperture blackbody in a range of temperature wide enough to cover the surface temperature conditions in the field. The accuracies of thermistors, TIR radiometers and spectrometer are better than 0.5 °C.

Spectral directional-hemispherical emissivity can be measured with an integrating sphere facility which includes a Fourier transform infrared (FTIR) spectrometer and a 5-inch infragold integrating sphere. The spectrometer has sensitivity both in the mid and thermal infrared, covering all MODIS bands of interest for LST. This instrument is primarily used for emissivity measurements of samples such as ice, water, silt, sand, soil, leaf surface, and etc. The surface roughness of these samples is limited to a few millimeters. Laboratory and field measurements of the infrared BRDF (bidirectional reflectance distribution function) and emissivity can also be made with the UCSB SIBRE (Spectral Infrared Bidirectional Reflectance and Emissivity) instrument, which includes a hemispherical pointing system, FTIR spectrometer, a TIR source, and reference plates (Snyder et al, 1997b). The effect of surface temperature change due to the thermal source heating is carefully corrected (Snyder and Wan, 1996). The spot size viewed by the MIDAC spectrometer is approximately 3cm in diameter so materials with some small-scale surface structure can be examined. We also have a beam expander that gives a 12cm spot for more structured surfaces. We can recover angular spectral emissivity (but not BRDF) from absolute radiance measurements using a sun-shadow technique which is similar to the day/night method.

### 4. PRELIMINARY RESULTS

The surface temperature and emissivity values retrieved from MAS data were compared with well calibrated in-situ data from the TIR scanning spectrometer, radiometers, and thermistors as shown in Table III. The LST value retrieved from MAS data acquired in MAS mission 1D is obtained with the generalized split-window LST method because there was only a daytime MAS flight mission for this first EOS Calibration/Validation field

campaign. In this case, the emissivity values for the split-window channels are obtained by the measurements of surface samples with the integrating sphere facility in laboratory. For other six MAS flight missions listed in Table III, the LST values retrieved from MAS data are obtained with the day/night LST algorithm. Co-registration of the day and night MAS images is necessary for the day/night LST algorithm. Because the day and night MAS data were acquired by the same ER-2 aircraft flying at almost the same altitude and flight direction in the day and night flight missions, the high quality of the MAS images made it relatively easy for us to do the co-registration. After we enhance the MAS images in a few channels with the histogram equalization method, we can find ground control points (roads and river streams) on both the day and night MAS images. Then we can make co-registration of the night MAS image with the day MAS image by shifting certain numbers of lines and samples that are determined by the pairs of ground control points. We can check the quality of the co-registration by overlaying a transparency sheet of the day MAS image on the another sheet for the night MAS image. The uncertainty in day/night co-registration is approximately a few MAS pixels. In order to increase the signal-to-noise ratio of the MAS data and to reduce the effect of the error in co-registration, we average the MAS data for every 2 by 2 pixels before applying the day/night LST algorithm. For all test sites where we made ground-based measurements under clear-sky conditions during MAS overflights, the LST values retrieved from MAS data agreed with those from field measurements within 1 °C. Band emissivities retrieved from MAS data agreed well with generalized geological maps. The topographic map (series no. NJ11-11) and the generalized geological map (Crowley and Hook, 1996) of Death Valley, CA are shown in Fig. 1. The daytime and nighttime LST images and band emissivities in MAS channels 30 and 42 retrieved from MAS data for Death Valley on 3 and 4 April 1997 are shown in Fig. 2. There are obvious topographic features in the daytime and nighttime (18:50 PST) LST images, but not in the emissivity images. It is observed that the band emissivities retrieved from MAS data agreed well with the generalized geological map.

Fig. 3 shows the LST and emissivity images retrieved from MAS data for Railroad Valley, NV on 23 and 24 June 1997. It is worthwhile to point out that we observed the spatial variation in the playa surface temperature with both MAS data and field measurement data. For the three field campaigns we conducted in 1995-1997, the brightness temperature images of MAS data in the channels at 11  $\mu\text{m}$  and the LST images retrieved from MAS data with the MODIS LST algorithms show that the standard deviation in playa surface temperature is approximately 1 °C and 0.5 °C in day and at night, respectively. There is always a large variation in the daytime surface temperature because of the solar forcing and the large variation in the surface wind speed during the day. The surface wind is usually calm during night. This makes it relatively easy to make field measurements of the LST at night and the accuracy of the LST from field measurements at night is higher.

Note that the grey level scales for LST and band emissivity images in Fig. 2 and Fig. 3 are fixed at the same values (0-255 corresponding to temperature range from -5.0 to 58.75 °C in steps of 0.25 °C, and 0-255 corresponding to emissivity range from 0.49 to 1.0 in steps of 0.002). It is reasonable that the overall day and night LST values are higher in Railroad Valley in June than those in Death Valley in early March. However, the surface emissivity in Death Valley varies in a much wide range than in Railroad Valley both in MAS channels 30 and 42. There is less contrast in the channel 42 emissivity images in both Fig. 2 and Fig. 3 because the band-averaged emissivity in channel 42 varies in a narrow range. These generally agree with the emissivity features obtained from our laboratory measurements and literature (Salisbury and D'Aria, 1992 and 1994).

## 5. ACTIVITIES IN THE NEAR FUTURE

The results from our previous field campaigns indicate that the spatial variation in field measurement data is the major source of the uncertainty in the LST validation. Recently we have made a great effort to reduce this uncertainty. We purchased 12 Heimann radiometers with a special window filter of 10-13  $\mu\text{m}$ . The effect of the large variation in emissivity below 10  $\mu\text{m}$  can be reduced by the use of this filter. We expect that the accuracy of the LST measurements can be improved by averaging the LST values from 12 Heimann radiometers well distributed over an area of 100 by 100m or 1 by 1km for comparison with LST values retrieved from MAS or MODIS data. We also purchased an IR camera from AGEMA Infrared Systems. There are 240 by 320 elements in this uncooling microbolometer-based IR camera. So we can easily place this IR camera on towers, low-level aircraft or balloons for measuring the temporal spatial LST distribution over test sites. Further improvements have been made to the existing scanning TIR spectrometer. The number of blackbodies in the front of the spectrometer is increased from two to four. One of the blackbodies is at the ambient temperature ( $T_{am}$ ), the second one at a temperature approximately 10 °C above  $T_{am}$ , the third one at 20 °C above  $T_{am}$ , and the fourth one

at 10-15 °C below  $T_{am}$ . In this way, we can reduce the calibration error due to the non-linearity in the spectrometer response and reach the accuracy of 0.2 °C in the spectral ranges where the seven MODIS bands used in the MODIS LST algorithm are located. The spot size of the field-of-view of the scanning spectrometer is increased to 36cm from 12cm by placing it on a support structure 3m above the ground instead of 1m so that the surface sample measured by the spectrometer will better represent the surface condition of the test sites.

We plan to deploy these new and improved instruments in the field campaigns at Mammoth Lake and Death Valley, CA scheduled in late February and early March 1998. A post-launch field campaign at Railroad Valley, NV is also planned for late September 1998 so that we can validate the MODIS LST algorithm using real MODIS data in its early stage. ER-2 MAS will fly for these two field campaigns. We plan to make more sun-shadow measurements before and after MAS/MODIS overflights during these two field campaigns in order to validate the emissivity retrieval.

## ACKNOWLEDGEMENTS

This work was supported by EOS Program contract NAS5-31370 of the National Aeronautics and Space Administration. The authors wish to express their gratitude to Bill Collette and Jeff Myers, NASA Ames Research Center, for the ER-2 flights and MAS data, to Richard Martin, Death Valley National Park, for research/collecting permit for our field campaign in March 1997, and to Chris Moeller and Liam Gumley, SSEC/CIMSS, for providing the MAS spectral response functions in digital form.

## REFERENCES

- Crowley, J. K. and S. J. Hook, "Mapping playa evaporite minerals and associated sediments in Death Valley, California, with multispectral thermal infrared images," *J. Geophys. Res.*, vol. 101, no. B1, pp. 643-660, 1996.
- King, M. D., D. D. Herring, and D. J. Diner, "The Earth Observing System (EOS): A space-based program for assessing mankind's impact on the global environment," *Opt. Photo. News*, vol. 6, pp. 34-39, 1995.
- King, M. D., W. P. Menzel, P. S. Grant, J. S. Myers, G. T. Arnold, S. E. Platnick, L. E. Gumley, S. C. Tsay, C. C. Moeller, M. Fitzgerald, K. S. Brown, and F. G. Osterwisch, "Airborne scanning spectrometer for remote sensing of cloud, aerosol, water vapor and surface properties," *J. Atmos. Ocean. Technol.*, vol. 13, pp. 777-794, 1996.
- Salisbury, J. W. and D. M. D'Aria, "Emissivity of terrestrial materials in the 8-14  $\mu\text{m}$  atmospheric window," *Remote Sens. Environ.*, vol. 42, pp. 83-106, 1992.
- Salisbury, J. W. and D. M. D'Aria, "Emissivity of terrestrial materials in the 3-5  $\mu\text{m}$  atmospheric window," *Remote Sens. Environ.*, vol. 47, pp. 345-361, 1994.
- Salomonson, V., W. Barnes, P. Maymon, H. Montgomery, and H. Ostrow, "MODIS: advanced facility instrument for studies of the Earth as a system," *IEEE Trans. Geosci. Remote Sens.*, vol. 27, no. 2, pp. 145-153, 1989.
- Snyder, W. and Z. Wan, "Surface temperature correction for active infrared reflectance measurements of natural materials," *Appl. Optics*, vol. 35, no. 13, pp. 2216-2220, 1996.
- Snyder, W., Z. Wan, Y. Zhang, and Y.-Z. Feng, "Requirements for satellite land surface temperature validation using a silt playa," *Remote Sens. Environ.*, vol. 61, pp. 279-289, 1997a.
- Snyder, W., Z. Wan, Y. Zhang, and Y.-Z. Feng, "Thermal infrared (3-14  $\mu\text{m}$ ) bidirectional reflectance measurements of sands and soils," *Remote Sens. Environ.*, vol. 60, pp. 101-109, 1997b.
- Wan, Z. and J. Dozier, "A generalized split-window algorithm for retrieving land-surface temperature from space," *IEEE Trans. Geosci. Remote Sens.*, vol. 34, no. 4, pp. 892-905, 1996.
- Wan, Z. and Z.-L. Li, "A physics-based algorithm for retrieving land-surface emissivity and temperature from EOS/MODIS data," *IEEE Trans. Geosci. Remote Sens.*, vol. 35, no. 4, pp. 980-996, 1997.

TABLE I. The central wavelength ( $\lambda_c$ ) and bandwidth ( $\Delta\lambda$ ) of MODIS Airborne Simulator (MAS) channels as configured in June 1997 and the equivalent channels of the MODIS onboard the EOS AM-1 platform to be launched in June 1998.

MAS channel	$\lambda_c$ ( $\Delta\lambda$ ) $\mu\text{m}$ (nm)	MODIS channel	$\lambda_c$ ( $\Delta\lambda$ ) $\mu\text{m}$ (nm)	MAS channel	$\lambda_c$ ( $\Delta\lambda$ ) $\mu\text{m}$ (nm)	MODIS channel	$\lambda_c$ ( $\Delta\lambda$ ) $\mu\text{m}$ (nm)
1	0.47 (39)	3	0.47 (20)	26	3.12 (155)		
2	0.55 (42)	4	0.56 (20)	27	3.28 (149)		
3	0.65 (52)	1	0.65 (50)	28	3.44 (159)		
4	0.70 (43)	14	0.68 (10)	29	3.58 (154)		
5	0.74 (42)	5	0.75 (10)	30	3.74 (140)	20	3.79 (180)
6	0.82 (44)			31	3.90 (152)	22	3.97 (59)
7	0.87 (42)	2	0.86 (35)	32	4.05 (151)	23	4.06 (61)
8	0.91 (41)	17	0.91 (30)	33	4.23 (157)		
9	0.95 (41)	19	0.94 (15)	34	4.38 (165)	24	4.47 (65)
10	1.63 (52)	6	1.64 (25)	35	4.54 (149)	25	4.55 (67)
11	1.68 (52)			36	4.68 (158)		
12	1.74 (52)			37	4.84 (149)		
13	1.79 (52)			38	5.00 (142)		
14	1.84 (50)			39	5.16 (145)		
15	1.89 (52)			40	5.29 (142)		
16	1.94 (52)			41	5.40 (93)		
17	1.99 (54)			42	8.59 (302)	29	8.54 (300)
18	2.04 (57)			43	9.66 (529)	30	9.73 (300)
19	2.09 (55)			44	10.49 (440)		
20	2.14 (56)	7	2.13 (50)	45	10.99 (490)	31	11.01 (500)
21	2.19 (55)			46	11.98 (420)	32	12.03 (500)
22	2.24 (57)			47	12.87 (410)		
23	2.29 (55)			48	13.29 (460)	33	13.36 (300)
24	2.33 (56)			49	13.83 (560)	35	13.91 (300)
25	2.38 (56)			50	14.28 (430)	36	14.19 (300)

TABLE II. The MAS flight missions and field measurements conducted for the validation of MODIS LST algorithms in 1995-1997.

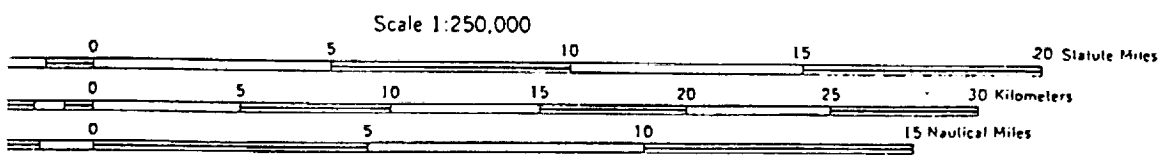
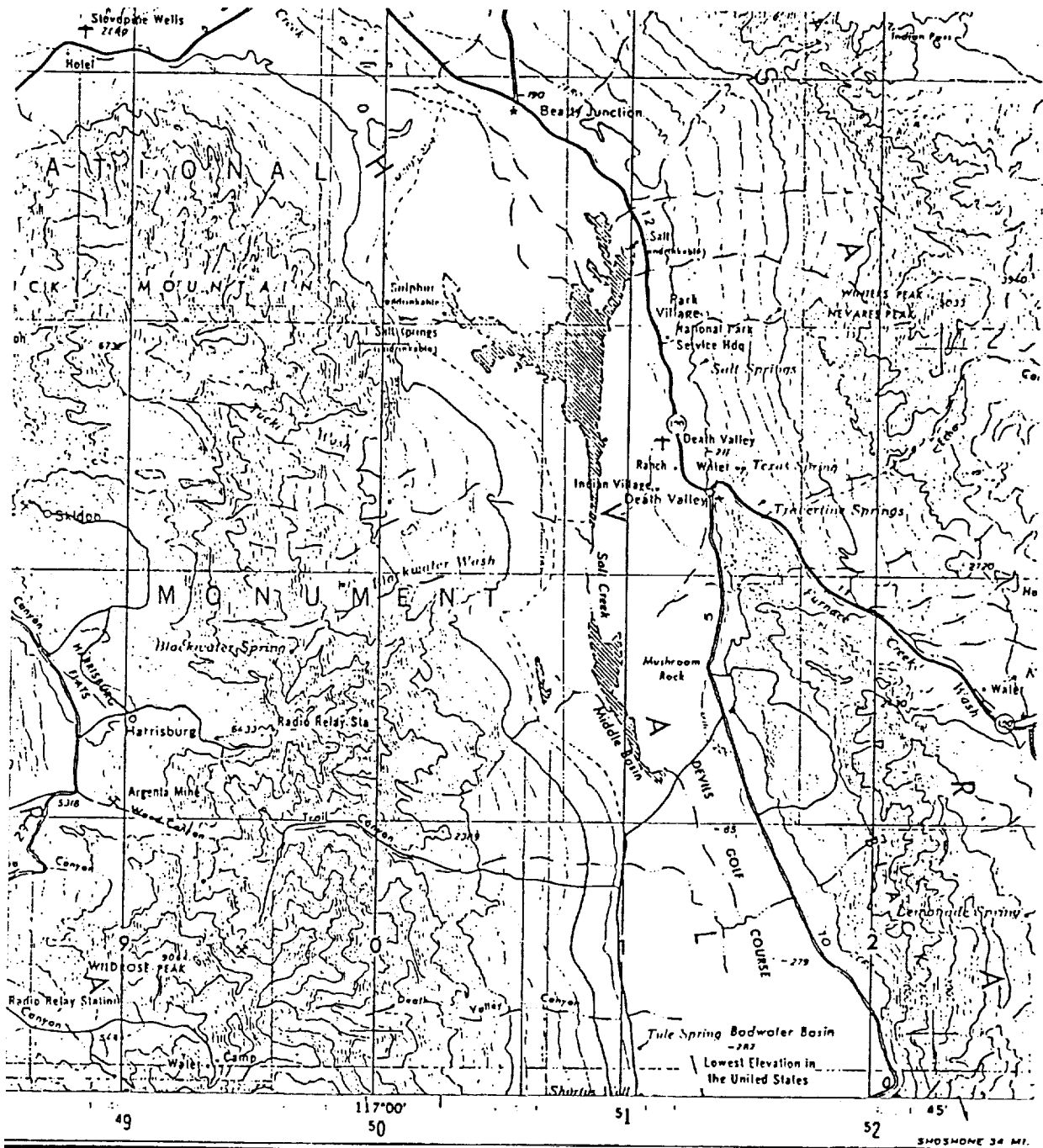
mission	test site	date	time (PST)	field measurements			weather conditions
				E1	E2	E3	
1D	Railroad Valley, NV	3 Aug 1995	12:58-13:45	1	1	0	clear-sky, broken clouds
2D	Mammoth Lake, CA	2 Apr 1996	13:31-14:12	1	1	1	partly cloudy
2N	Mammoth Lake, CA	3 Apr 1996	18:31-19:12	1	1	1	partly cloudy
3D	Railroad Valley, NV	4 Jun 1996	10:53-11:59	1	1	1	clear-sky, $cwv \approx 1.4\text{cm}$
3N	Railroad Valley, NV	5 Jun 1996	18:50-19:37	1	1	1	clear-sky
4D	Death Valley, CA	3 Mar 1997	12:32-13:05	1	2	9	clear-sky, $cwv \approx 0.5\text{cm}$
4N	Death Valley, CA	4 Mar 1997	18:43-19:04	1	2	9	clear-sky
5D	Railroad Valley, NV	23 Jun 1997	9:30-10:42	1	2	7	clear-sky, $cwv \approx 0.7\text{cm}$
5N	Railroad Valley, NV	24 Jun 1997	18:30-19:30	1	2	10	clear-sky, $cwv \approx 0.7\text{cm}$

Note: E1 stands for TIR spectrometer, E2 for TIR thermometer, E3 for thermistor 1mm beneath the surface.

TABLE III. The summary of LST values retrieved from MAS data and field measurement data under clear-sky conditions in the LST field campaigns in 1995-1997.

mission	test site latitude, longitude	date	time (PST)	Ts (MAS)	Ts (field measurements)		
				(°C)	E1	E2	E3
1D	38° 31.46'N, 115° 42.74'W	3 Aug 1995	13:26	[59.1]	59.2	58.5	
3D	38° 27.69'N, 115° 41.50'W	4 Jun 1996	11:25	57.7	57.5	56.7	56.0
3N	38° 27.69'N, 115° 41.50'W	5 Jun 1996	18:55	24.8	24.2	24.8	24.4
4D	36° 21.12'N, 116° 51.36'W	3 Mar 1997	12:39	41.3		41.8, 42.1	40.6
4N	36° 21.12'N, 116° 51.36'W	4 Mar 1997	18:50	18.6		18.4, 18.9	18.5
5D	38° 27.72'N, 115° 41.57'W	23 Jun 1997	10:11	46.5	46.0	47.1	46.5
5N	38° 27.72'N, 115° 41.57'W	24 Jun 1997	18:59	22.5	22.8	22.3	23.1

Note: The uncertainties in  $T_s$  values calculated from TIR spectrometer (E1) and thermometer (E2) data are approximately 0.5°C due to the errors in instrument calibration and in the surface emissivity values used. The thermistor datalogger (E3) has an accuracy better than 0.5°C, but it does not give the temperature at surface.



CONTOUR INTERVAL 200 FEET  
WITH SUPPLEMENTARY CONTOURS AT 100 FOOT INTERVALS

MAGNETIC DECLINATION FOR 1970 IS 15W\* (280 MILS) EASTERLY OVER THE ENTIRE AREA

BY U. S. GEOLOGICAL SURVEY, DENVER, COLORADO 80225, OR RESTON, VIRGINIA 22092

Fig. 1, (a) Topographic map of Death Valley, California,

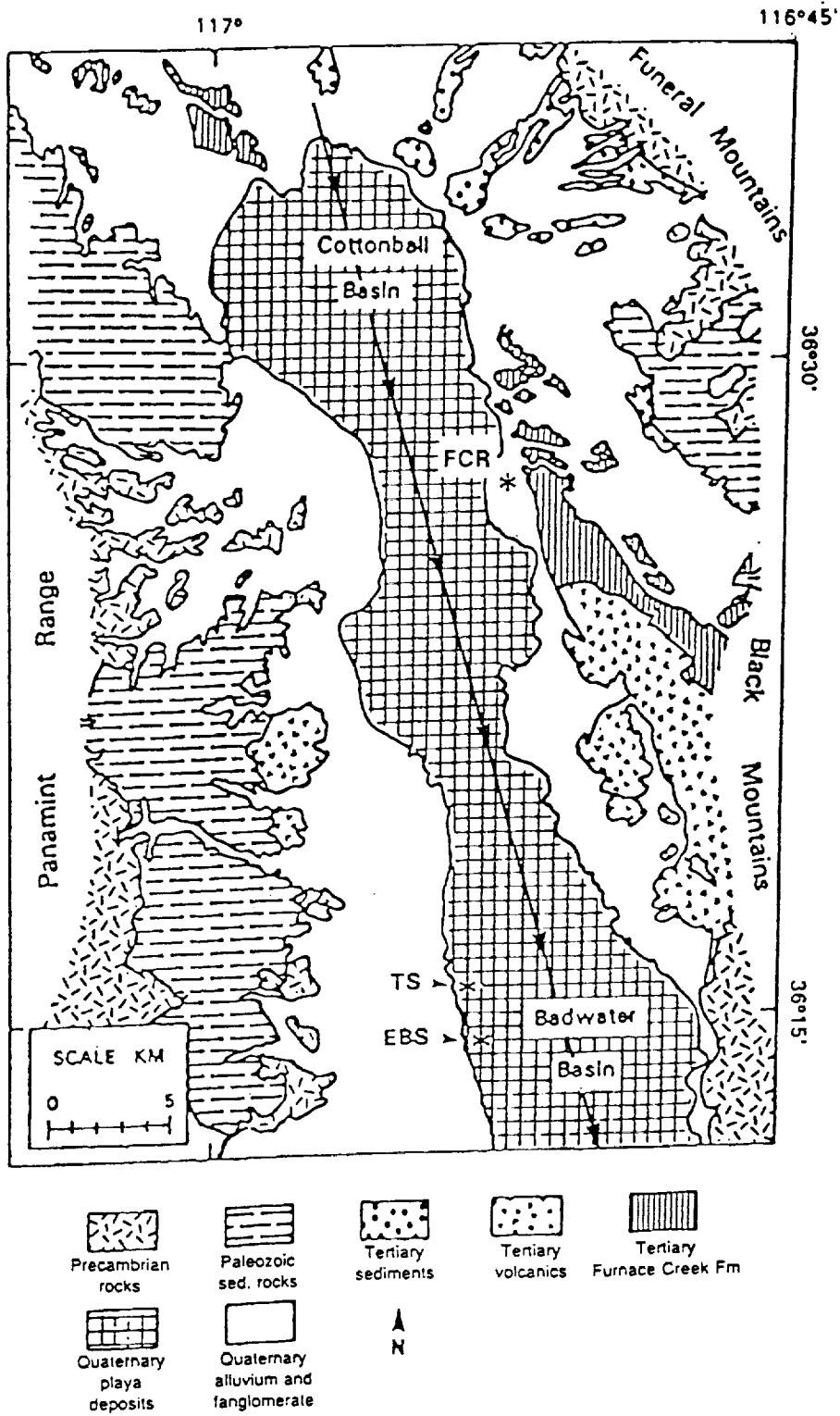
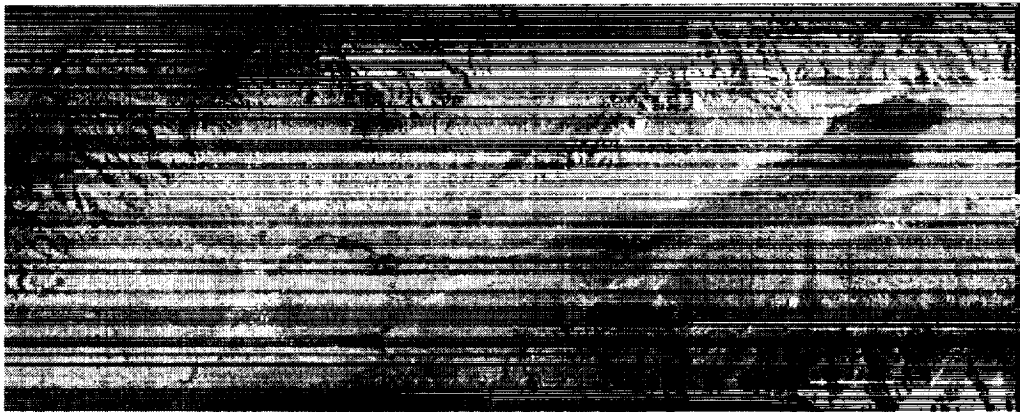
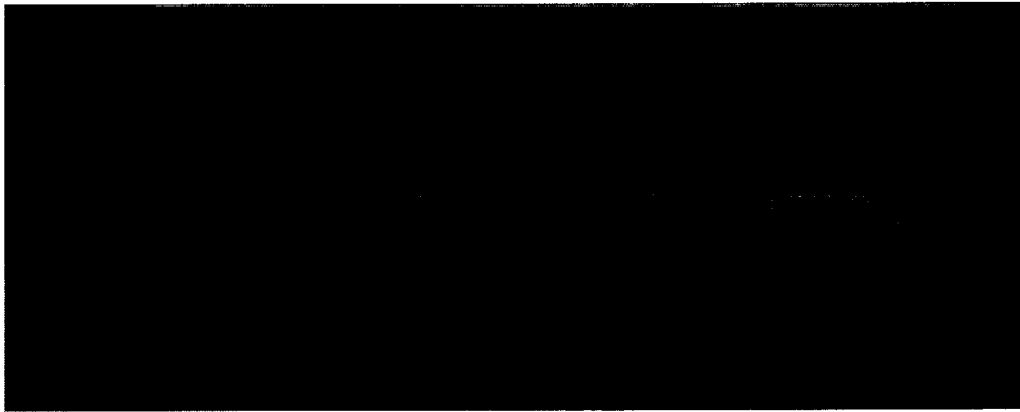


Fig. 1 (continued), (b) generalized geological map (Crowley and Hook, 1996).

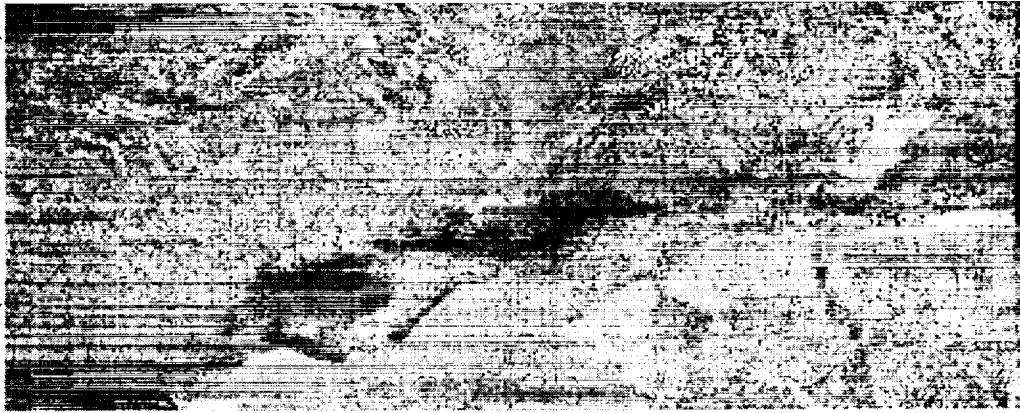
LST 12:39 PST 3/3/97



LST 18:50 PST 3/4/97



em(band 30, 3.73mu)



em(band 42, 8.53mu)



Fig. 2, Land-surface temperature and emissivities retrieved from MAS data at Death Valley, CA.

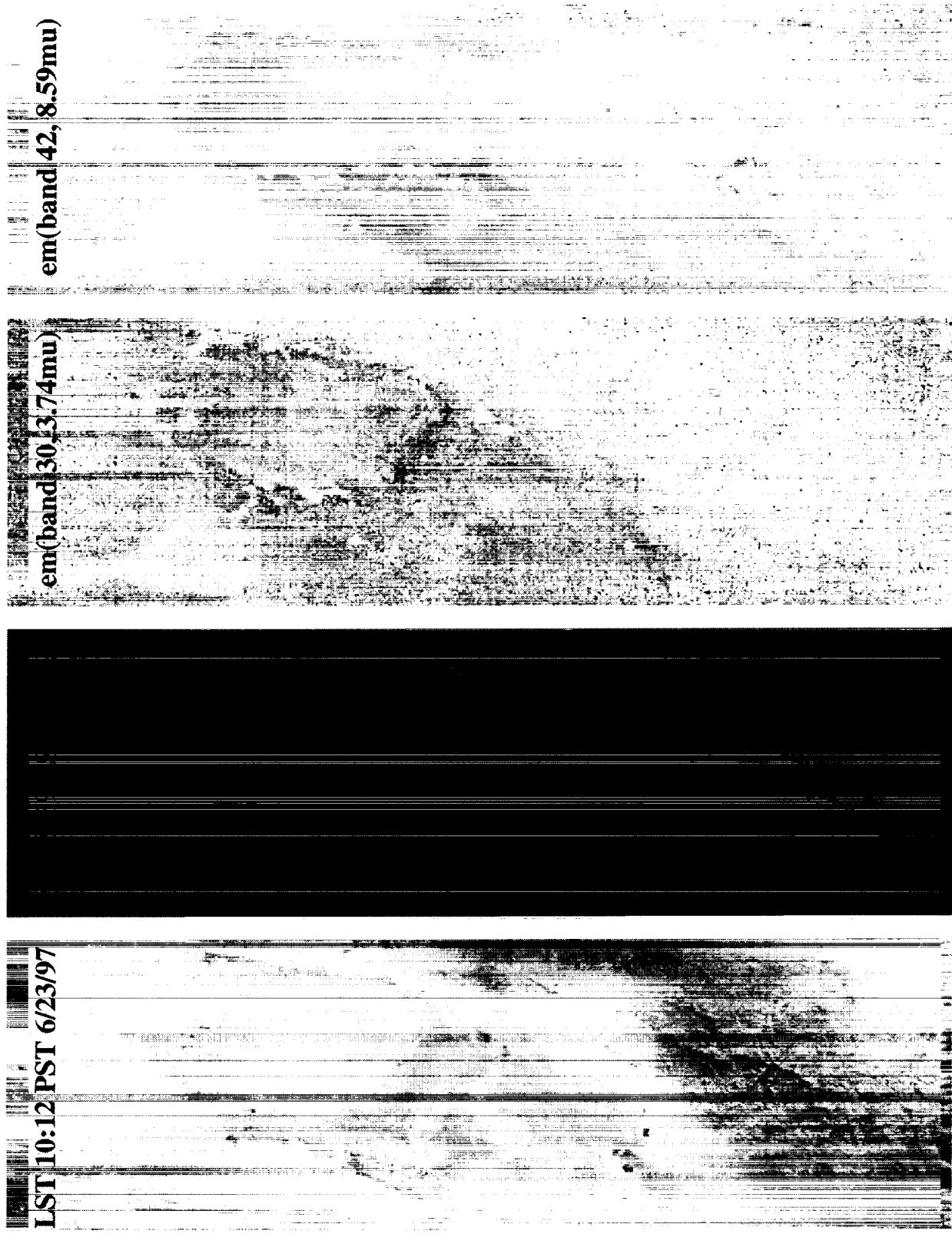


Fig. 3, Land-surface temperature and emissivities retrieved from MAS data at Railroad Valley, NV.